EAI Endorsed Transactions
on Industrial Networks and Intelligent Systems
Research Article EAI.EU

Real-time Single-Channel EOG removal based on Empirical Mode Decomposition

Nguyen Trong Kien[1,*], Nguyen Luong Nhat[1], Tan Hanh[1], Tran Trung Duy[1], Ha Thi Thanh Huong[2], Pham The Duy[1], Nguyen Thanh Binh[1]

[1]Posts and Telecommunications Institute of Technology, Ho Chi Minh City, Vietnam.
[2]International University, Ho Chi Minh City, Viet Nam.

Abstract

In recent years, single-channel physiological recordings have gained popularity in portable health devices and research settings due to their convenience. However, the presence of electrooculogram (EOG) artifacts can significantly degrade the quality of the recorded data, impacting the accuracy of essential signal features. Consequently, artifact removal from physiological signals is a crucial step in signal processing pipelines. Current techniques often employ Independent Component Analysis (ICA) to efficiently separate signal and artifact sources in multichannel recordings. However, limitations arise when dealing with single or a few channel measurements in minimal instrumentation or portable devices, restricting the utility of ICA. To address this challenge, this paper introduces an innovative artifact removal algorithm utilizing enhanced empirical mode decomposition to extract the intrinsic mode functions (IMFs). Subsequently, the algorithm targets the removal of segments related to EOG by isolating them within these IMFs. The proposed method is compared with existing single-channel EEG artifact removal algorithms, demonstrating superior performance. The findings demonstrate the effectiveness of our approach in isolating artifact components, resulting in a reconstructed signal characterized by a strong correlation and a power spectrum closely resembling the ground-truth EEG signal. This outperforms the existing methods in terms of artifact removal. Additionally, the proposed algorithm exhibits significantly reduced execution time, enabling real-time online analysis.

Keywords: Empirical mode decomposition, electrooculogram artifacts, single-channel artefact removal

Received on 13 December 2023, accepted on 25 March 2024, published on 08 April 2024

doi: 10.4108/eetinis.v11i2.4593

*Corresponding author. Email: kiennt021186@gmail.com

1. Introduction

Measurement of the various physiological signals in the human brain is a crucial process in assessing an individual's well-being. Electroencephalography (EEG) represents a non-linear and non-stationary electrophysiological signal of the central nervous system, providing comprehensive insights into brain activity. EEG data serves as a vital resource for human brain research, disease diagnosis, and rehabilitation engineering. Despite its significance, EEG data is highly vulnerable to external interference, such as electrooculogram EOG [1], electromyogram (EMG) [2] and electrocardiogram (ECG) artifacts [3]. These artifacts severely compromise EEG recording quality, potentially leading to misinterpretation of neural information [4]. Consequently, noise cancellation becomes a crucial pre-processing step for EEG data, ensuring accurate analysis and interpretation. Moreover, in recent years, EEG signal acquisition devices have become more portable and user-friendly, especially with the growing prevalence of brain-computer interfaces (BCIs) [5], [6], [7], [8]. There is a rising demand for fewer channels in specific applications such as portable anaesthesia depth monitoring and portable emotional state recognition [9], and portable sleep monitoring [10], where a single channel suffices for the intended purpose. This evolution underscores the need for advanced noise cancellation techniques, enabling precise EEG data analysis despite challenging recording conditions.

The commonly utilized filters are frequently employed for artifact removal in cases where there are non-overlapping frequency bands between signals and interferences. However, optimizing the bandwidth selection of these filters has proven challenging due to the nonlinear and nonstationary nature of EEG signals. Furthermore, separating noise becomes challenging when there is spectral overlap between brain signals and interferences. To address these challenges, more sophisticated algorithms like blind source separation (BSS), adaptive filtering, wavelet decompositions (WT), and empirical mode decomposition (EMD) have been proposed to efficiently eliminate interferences from EEG signals [11], [12], [13], [14], [15], [16], [17]. One popular BSS technique, independent component analysis (ICA), effectively separates multi-channel EEG signals into independent components, comprising both sources and artifacts [18], [19]. By removing artifact-related independent components (ICs), clean EEG signals can be reconstructed. However, BSS-based methods are effective only when the number of EEG channels is sufficiently large.

While several methods have been suggested to effectively eliminate EOG signals [18], [20], [21], [22], [23], [24], these techniques pose challenges when applied to single-channel portable BCI systems, as they typically require multiple EEG channels for optimal separation. Kumar introduced an approach in 2008 that employs wavelet transform soft thresholding to remove single-channel EOG artifacts [24]. However, this method demands substantial prior knowledge and adversely affect EEG source signal components. Although source separation techniques require multiple channels, they can be used on a single-channel in association with WT or EMD [12], [25]. Mammone proposed a WT-ICA algorithm in 2012, combining wavelet transform and independent component analysis to eliminate EOG artifacts [11], [25]. For example, wavelet transform has been applied as a bandpass filter to decompose the single-channel biomedical signal into several components. The ICA is then employed on these decomposed components to extract the sources and eliminate the artifacts [12]. This algorithm satisfies the ICA a priori condition through wavelet decomposition of single-channel EEG signals. Nevertheless, the performance of wavelet transform mainly depends on the selection of wavelet kernel functions. In addition, the wavelet transform not only increases observed signals but also decomposes the source signal into several sub-source signals. An alternating decomposition method, empirical mode decomposition is an adaptive method capable of handling non-linear and non-stationary signals more effectively by decomposing the signal into single modes, known as intrinsic mode functions, without linearity assumptions [26]. That is, each successive EMD will generate an IMF with lower oscillations than the previous IMF and naturally retain the physical properties of the signal. Later, ICA is applied on the IMFs to extract the hidden sources. However, the EMD may produce the disparated frequency bands in one IMF or similar oscillation in different IMFs, known as “mode-mixing”. Thus, for resolving a mode-mixing problem when using EMD, an extended noise-assisted method known as the ensemble EMD (EEMD) was developed [27]. Later, the EEMD-based methods such as Complete ensemble empirical mode decomposition have been developed and proved to be efficiently decompose biomedical signals [28], [29]. Although these decomposition methods have been previously employed as useful methods to decompose the single channel EEG signal into components consisting signals and undesired noises, the repetitive number of ensemble of EEMD-based methods causes the intensive computation and is thus not suitable for the real-time system. Additionally, a significant limitation of source separation techniques like ICA is their inability to be applied online [14]. While some real-time applications have been proposed by computing ICA on a sliding window in a recurrent manner [30], [31] there is currently no efficient online algorithm available. Furthermore, the effectiveness of ICA is influenced by the length of the signal [32]. That is too short can hinder the reliable separation of sources, while an excessively long signal can lead to changes in the properties of the sources over time, resulting in improper isolation of artifacts. These constraints render ICA and similar BSS-based methods impractical for real-time continuous monitoring scenarios.

In this article, we introduce a highly effective approach for removing the EOG artifact from a single-channel EEG signal. Our method utilizes an enhanced empirical mode decomposition technique, specifically the masking EMD, associated with EOG detection based on the envelope of each intrinsic mode function to remove the EOG artifact. To gauge its performance, we conducted a comparative analysis with existing removal methods, namely VMD-SOBI [33] and EEMD-ICA [12]. In Section II, we offer a concise overview of our proposed methods. Section III presents a detailed comparison of the outcomes obtained from these techniques. Finally, in Section IV, we provide a conclusion based on the obtained results.

2. Methods

2.1. Empirical Mode Decomposition (EMD)

EMD stands out as an adaptive and data-driven methodology that operates without the constraints of linearity assumptions. It dynamically decomposes the characteristics of raw signals into individual modes called intrinsic mode functions, all without the need for predetermined band-pass filter cut-offs. Consequently, each EMD algorithm functions as a natural dyadic filtering bank [34], as described in the following equation:

$$x(t) = \sum_{j=1}^{n} IMF_j(t) + r(t) \quad (1)$$

Let x(t) be the input data, the following steps outline the process used to identify Intrinsic Mode Functions:

1. Identify time-series local maxima and minima of x(t)

2. Perform a cubic spline interpolation between all local maxima to compute the upper envelope $e_{max}(t)$ and the lower envelope $e_{min}(t)$.
3. Estimate the mean value of each data time-point between the upper and lower envelope as $m_1(t) = (e_{max}(t) + e_{min}(t))/2$
4. Subtract the mean value from the original signal to provide the local components $h_1(t) = X(t) - m_1(t)$.
5. The sifting procedure was implemented to ensure that the component $h_1(t)$ met the criteria to be classified as an Intrinsic Mode Function. The stopping criterion for the sifting process is defined in Equation (2), calculated from the two consecutive components as:

$$\delta_m = \sum_{t=0}^{N} \frac{\left|h_{1(m-1)}(t) - h_{1(m)}(t)\right|^2}{h^2{}_{1(m-1)}(t)} \quad (2)$$

A threshold value for δ (i.e., standard deviation) can be set between 0.2 and 0.3 to stop the sifting process [35]. The process is reiterated until only a monotonic time-series or residue r(t) remains, signifying the underlying trend within x(t).

To enhance the decomposition process and mitigate mode-mixing issues inherent in the original EMD, an improved algorithm called masking EMD was employed [36], [37], [38], [39]. Masking EMD robustly decomposes the signal into physically meaningful nonlinear components, as demonstrated in prior research [39]. A notable advantage of masking EMD is its ability to extract intrinsic mode functions (IMFs) without the need for a specified number of iterations, which significantly reduces computational costs and enhances execution speed. Thus, it is a crucial step toward efficient real-time EOG artifact removal in practical applications.

2.2. The proposed algorithm

In conventional approaches, the decomposition process is followed by the application of ICA-based methods to eliminate EOG-related components. However, a significant drawback of source separation techniques like ICA is their limited applicability in real-time scenarios. Moreover, the performance of ICA is adversely affected by signal length, leading to improper isolation of artifacts.

The proposed algorithm addresses these challenges by efficiently detecting and removing only the EOG-related segments from the signal, with minimal execution time for online applications. The algorithm comprises three key steps: 1. Decomposition: Raw signals are decomposed into components.; 2. Detection: EOG-related segments are identified within these components.; 3. Removal and Reconstruction: The EOG-related segments are removed, and the clean signal is reconstructed. The details of analysis flow were conducted as follows:

1. The original signal x(t) is firstly decomposed into several IMFs by using masking EMD, with these known as the first layer IMFs.
2. Then the Hilbert transform method is applied to estimate instantaneous frequencies and amplitudes of the IMFs. This step gives the time-frequency characteristics of the original signal and is known as the Hilbert-Huang Transform (HHT). The mean instantaneous frequencies were calculated to define the low-frequency IMF ranging from 0.5 to 8 Hz since those IMFs include strong amplitude of EOG signal.

3. Construct the envelop of each given low-frequency IMFs by using the instantaneous amplitudes of IMFs extracted by Hilbert transform.

4. At the low-frequency IMFs, the EOG amplitude is typically dominant and lasts for about 1 second. Thus, we define the 1-s segment of EOG signal in low-frequency IMFs using a threshold of 2 times the standard deviation of entire signal. Then, we replace those EOG segments by zeroes from low-frequency IMFs.

5. After EOG segment removal, the clean signal is constructed by summing all the IMFs.

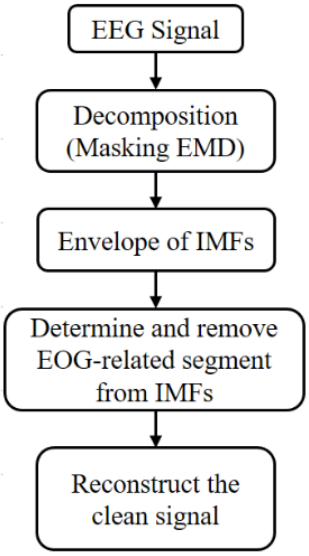

Figure 1. The flowchart of the proposed algorithm.

2.3. Dataset for Benchmarking

The Semi-Simulated EEG/EOG [40] includes 55 recordings obtained from 19 EEG electrodes, sampled at a frequency of 200 Hz. Each EEG recording is accompanied by an equal number of EOG signals. These EOG signals are incorporated

linearly into the EEG signal, leading to recordings affected by artifacts.

2.4. Performance Metrics

Correlation

In time domain, we used the Pearson correlation coefficient, which is a widely accepted measure of the statistical relationships between signals, to measure the linear temporal correlation between original signal and clean signal. We defined the change in correlation R as in Equation (3):

$$R = \frac{\sum_{i=1}^{n}(x_i - \bar{x})(y_i - \bar{y})}{\sqrt{\sum_{i=1}^{n}(x_i - \bar{x})^2}\sqrt{\sum_{i=1}^{n}(y_i - \bar{y})^2}} \quad (3)$$

Where $\bar{x}$ and $\bar{y}$ are the sample means of signal x and y, respectively.

Spectral Coherence

In EEG analysis, the majority of extracted features are derived from the frequency domain. Therefore, assessing the enhancement in spectral coherence before and after artifact removal is crucial to determine the efficacy of the artifact removal process. Evaluating the increase in spectral coherence between the clean signal and the original signal post-artifact removal serves as a significant metric [41]. This enhancement in coherence, denoted as I_{coh}, is defined as in Equation (4):

$$I_{coh} = \frac{(C_{\text{after}} - C_{before})}{(1 - C_{before})} \quad (4)$$

where C_{before} and C_{after} represent the average magnitude squared coherence estimates within the 1–10 Hz band. These values are computed by comparing the ground truth with the signal before and after artifact removal, respectively

Execution time

The execution time was determined by analyzing a 7-second sample at a sampling rate of 200 Hz using simulated data. Each method was iteratively applied to the identical dataset 10 times to calculate the average execution time. This metric holds significance as it assesses the ability of both the proposed and existing methods to operate in real-time scenarios. The benchmarks were conducted using Matlab 2015a, running on a system equipped with an AMD Ryzen 5 CPU (2.1 GHz) and 16 GB RAM.

3. Results

3.1 Application of the proposed method on Synthetic Signals.

In EEG signals, eye blink artifacts often manifest as spike-type signals. For our simulation study, we focused on separating mixed signals resembling these spike-type artifacts. To create this spike-type source signal, we first segmented a one-second eye blink epoch from a single-channel EEG recording in the Semi-Simulated EEG/EOG dataset. This segment was then positioned at 3.5 seconds alongside a segmented EOG in a zero-magnitude 7-second signal. The magnitudes of the EOG were rescaled to achieve various signal-to-noise ratios (SNR) ranging from -5 dB (representing a large artifact) to +5 dB (indicating a small artifact, as shown in Fig. 2). Finally, the simulated signal was constructed by adding the real EEG signal to the spike-type source signal at different SNR levels.

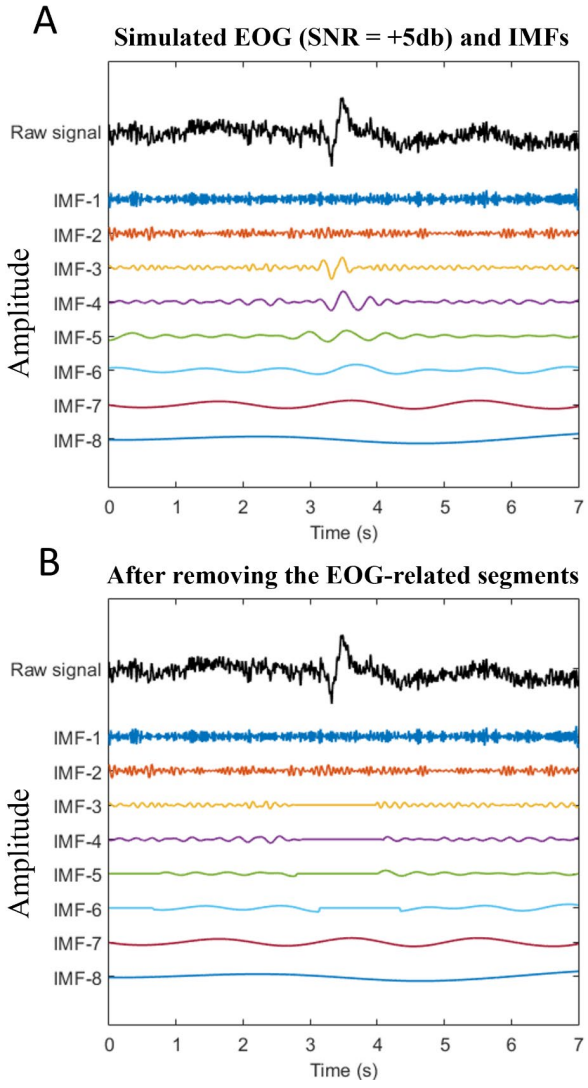

Figure 2. The illustration of EOG-related IMFs removal from a simulated signal (SNR = +5db).

Figure 2 illustrates the proposed method's process of decomposing raw data into Intrinsic Mode Functions and subsequently removing EOG-related segments from these IMFs. Initially, the raw data underwent decomposition using Masking Empirical Mode Decomposition (EMD), resulting in 8 IMFs (Figure 2A). Among these, IMFs 3, 4, 5, and 6 contained EOG-related components. The segments corresponding to EOG artifacts within these IMFs were accurately identified and replaced with zeroes, as shown in Figure 2B. The reduction in artifact components of the clean signal was measured through cross-correlation and enhancement in spectral coherence (I_{coh}), comparing the algorithm's output to the ground truth signal (refer to Figure 3 for details).

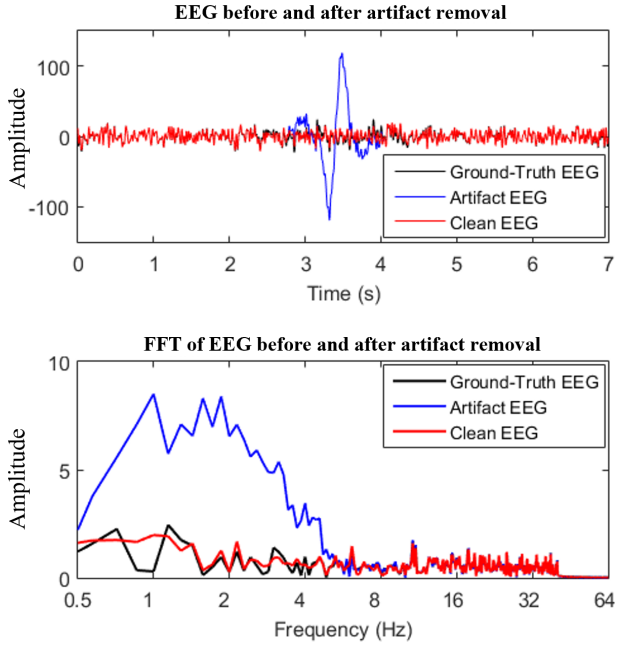

Figure 3. The clean signal reconstructed from a simulated signal and its power spectrum obtained by the proposed method.

The results obtained from our proposed method demonstrate its efficacy. The artifact-free EEG signals were reconstructed (indicated by the red line in Figure 3) with a strong correlation of 0.96 and 0.94 at SNR levels of +5dB and -5dB, respectively, compared to the ground truth signal. Furthermore, the method significantly improved spectral coherence, yielding I_{coh} values of 0.43 and 0.54 at +5dB and -5dB, respectively. These findings underscore the robustness and accuracy of our approach in artifact removal.

To further validate our approach, we conducted a benchmarking analysis, comparing it with alternative artifact removal algorithms suitable for single-channel EEG recordings, namely EMD-ICA and VMD-SOBI. Our findings revealed that our proposed method outperformed the other tested techniques in terms of correlation and spectral coherence. It consistently achieved the highest correlation and exhibited significant improvements in spectral coherence across various signal-to-noise ratios (see Figure 4). These results decisively confirm that our method preserves information in the time domain and avoids spectral distortion in the frequency domain.

Interestingly, the performance of the VMD-SOBI method showed similarities to our method in terms of correlation. However, it showed a low improvement of spectral coherence and similar to the results of EMD-ICA method. Moreover, the EMD-ICA method indicated a decline in correlation as the EOG artifact increased. This outcome serves as strong evidence that ICA and similar BSS methods might not be the most effective choices for removing the EOG artefact.

We compared the practical implementation performances of various algorithms by measuring the execution time required to analyze a 7-second data segment from the simulated data. The proposed method exhibited a mean execution time of 0.35 seconds, significantly outperforming VMD-SOBI (execution time = 7.6 seconds) and EMD-ICA (execution time = 1.1 seconds).

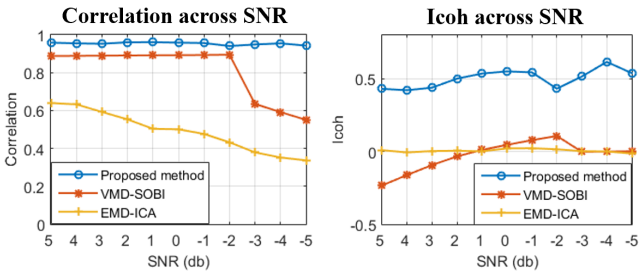

Figure 4. The performance of the proposed method comparing to two existing methods (VMD-SOBI and EMD-ICA)

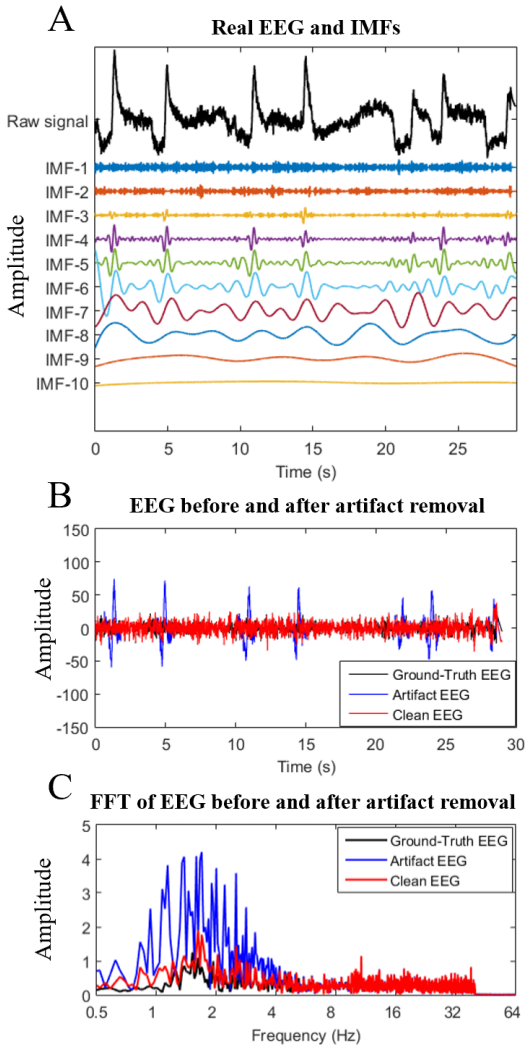

Figure 5. The illustration of analyzing a single subject from semi-EEG dataset. A. The decomposition of raw signal. B. The EEG signal before and after artifact removal. C. The power spectrum of ground-truth EEG, clean EEG and raw EEG.

In summary, our proposed method demonstrates superior performance compared to VMD-SOBI and EMD-ICA in terms of enhancing spectral coherence and reducing execution time. This improved performance is primarily attributed to the pivotal role of masking EMD, which serves as the initial step in decomposing single EEG channels. Our findings align with prior research indicating that masking EMD robustly decomposes signals into physically meaningful nonlinear components, surpassing the capabilities of original and ensemble EMD methods used in EMD-ICA [38], [39]. Additionally, the execution time of masking EMD is significantly lower than VMD decomposition utilized in VMD-SOBI, as shown in our result. By leveraging the robust decomposition capabilities of masking EMD, our innovative method precisely localizes the EOG segment using the envelope of each IMF, rather than relying on ICA or SOBI for artifact removal. This facilitates their direct removal without the necessity of discarding the entire decomposed signal and thus the computation cost is not highly required as in SOBI and ICA enabling it to apply in real time. As a result, our proposed approach has the potential to preserve vital EEG features, unlike VMD-SOBI and EMD-ICA.

3.2 Application of the proposed method on Semi-Simulated EEG/EOG dataset.

In the analysis of the semi-Simulated EEG/EOG dataset, our proposed method effectively eliminated EOG artifacts, resulting in clean EEG signals characterized by high correlation and a closely aligned power spectrum, especially within the EOG-related frequency range (0.5 Hz - 8 Hz), when compared to the ground-truth EEG, as demonstrated in the Figure 5. Furthermore, our method consistently outperformed both VMD-SOBI and EMD-ICA algorithms in terms of both correlation and spectral coherence across different subjects. As illustrated in the Figure 6, our method exhibited an average correlation value of 0.83 and an average spectral coherence of 0.05 across subjects. In terms of correlation, VMD-SOBI demonstrated a similar performance (mean correlation value = 0.77) to our proposed method, whereas EMD-ICA exhibited the lowest value of 0.42 across subjects.

4. Conclusion

In this study, we introduced and validated an innovative algorithm for removing EOG artifacts from single-channel EEG data in real-time. Our method, based on data-driven masking EMD, operates automatically without the need for auxiliary input, parameter tuning, or human intervention. Through testing, our approach consistently outperformed comparable algorithms relying on blind source separation, in both simulated and semi-simulated EEG data. Furthermore, our results demonstrated that our algorithm not only outperforms existing methods but also exhibits lower computational costs. Its performance remains robust for real-time applications, making it particularly valuable for studying cognitive functions and other specialized care unit applications where only a limited number of electrodes are available, and real-time analysis is essential. The enhanced spectral coherence achieved through our method ensures reliable reconstructed of clean signals, further emphasizing its suitability for such applications.

Additionally, our algorithm includes an automatic detection and removal feature for EOG artifacts, rendering it suitable for unsupervised EEG devices. These findings highlight the potential of our approach in advancing EEG artifact removal techniques for practical and real-time applications.

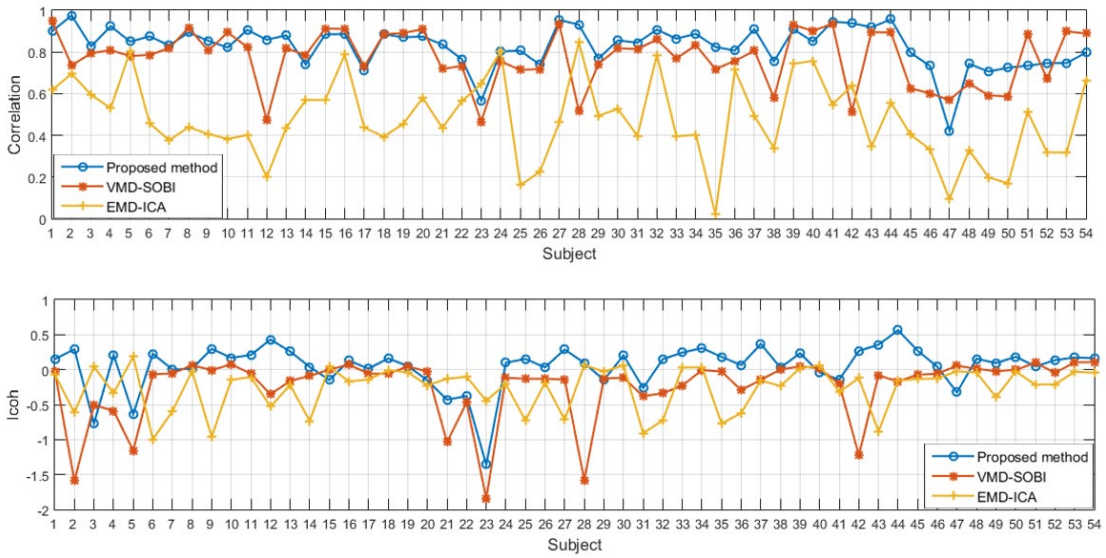

Figure 6. The performance of the proposed method and two existing methods across subjects in term of correlation and I_{coh} (improvement of spectral coherence).

Acknowledgements. This research is funded by Posts and Telecommunications Institute of Technology under grant number 14-2023-HV-ĐT2.

References

[1] M. Miao, W. Hu, B. Xu, J. Zhang, J. J. P. C. Rodrigues, and V. H. C. de Albuquerque, "Automated CCA-MWF Algorithm for Unsupervised Identification and Removal of EOG Artifacts From EEG," *IEEE J Biomed Health Inform*, vol. 26, no. 8, pp. 3607–3617, 2022, doi: 10.1109/JBHI.2021.3131186.

[2] L. Meng *et al.*, "Evaluation of decomposition parameters for high-density surface electromyogram using fast independent component analysis algorithm," *Biomed Signal Process Control*, vol. 75, p. 103615, 2022, doi: https://doi.org/10.1016/j.bspc.2022.103615.

[3] N. Mourad, "ECG denoising based on successive local filtering," *Biomed Signal Process Control*, vol. 73, p. 103431, 2022, doi: https://doi.org/10.1016/j.bspc.2021.103431.

[4] M. Klug and K. Gramann, "Identifying key factors for improving ICA-based decomposition of EEG data in mobile and stationary experiments," *European Journal of Neuroscience*, vol. 54, no. 12, pp. 8406–8420, Dec. 2021, doi: https://doi.org/10.1111/ejn.14992.

[5] G. Rebolledo-Mendez *et al.*, "Assessing NeuroSky's Usability to Detect Attention Levels in an Assessment Exercise," in *Human-Computer Interaction. New Trends*, J. A. Jacko, Ed., Berlin, Heidelberg: Springer Berlin Heidelberg, 2009, pp. 149–158.

[6] S.-F. Liang, C.-E. Kuo, Y.-H. Hu, Y.-H. Pan, and Y.-H. Wang, "Automatic Stage Scoring of Single-Channel Sleep EEG by Using Multiscale Entropy and Autoregressive Models," *IEEE Trans Instrum Meas*, vol. 61, no. 6, pp. 1649–1657, 2012, doi: 10.1109/TIM.2012.2187242.

[7] B. R. Greene, G. B. Boylan, W. P. Marnane, G. Lightbody, and S. Connolly, "Automated single channel seizure detection in the neonate," in *2008 30th Annual International Conference of the IEEE Engineering in Medicine and Biology Society*, 2008, pp. 915–918. doi: 10.1109/IEMBS.2008.4649303.

[8] S. Ge, R. Wang, and D. Yu, "Classification of Four-Class Motor Imagery Employing Single-Channel Electroencephalography," *PLoS One*, vol. 9, no. 6, pp. e98019-, Jun. 2014, [Online]. Available: https://doi.org/10.1371/journal.pone.0098019

[9] C. Wan, D. Chen, Z. Huang, and X. Luo, "A wearable head mounted display bio-signals pad system for emotion recognition," *Sensors*, vol. 22, no. 1, Jan. 2022, doi: 10.3390/s22010142.

[10] S. Kwon, H. Kim, and W.-H. Yeo, "Recent advances in wearable sensors and portable electronics for sleep monitoring," *iScience*, vol. 24, no. 5, p. 102461, 2021, doi: https://doi.org/10.1016/j.isci.2021.102461.

[11] G. Inuso, F. La Foresta, N. Mammone, and F. C. Morabito, "Wavelet-ICA methodology for efficient artifact removal from Electroencephalographic recordings," in *2007 International Joint Conference on Neural Networks*, 2007, pp. 1524–1529. doi: 10.1109/IJCNN.2007.4371184.

[12] B. Mijović, M. De Vos, I. Gligorijević, J. Taelman, and S. Van Huffel, "Source Separation From Single-Channel Recordings by Combining Empirical-Mode Decomposition and Independent Component Analysis," *IEEE Trans Biomed Eng*, vol. 57, no. 9, pp. 2188–2196, 2010, doi: 10.1109/TBME.2010.2051440.

[13] K. T. Sweeney, S. Member, S. F. McLoone, S. Member, and T. E. Ward, "The use of Ensemble Empirical Mode Decomposition with Canonical Correlation Analysis as a Novel Artifact Removal Technique."

[14] J. Yedukondalu and L. D. Sharma, "Circulant Singular Spectrum Analysis and Discrete Wavelet Transform for Automated Removal of EOG Artifacts from EEG Signals," *Sensors*, vol. 23, no. 3, Feb. 2023, doi: 10.3390/s23031235.

[15] C. Liu and C. Zhang, "Remove Artifacts from a Single-Channel EEG Based on VMD and SOBI," *Sensors*, vol. 22, no. 17, Sep. 2022, doi: 10.3390/s22176698.

[16] M. Wang, X. Cui, T. Wang, T. Jiang, F. Gao, and J. Cao, "Eye blink artifact detection based on multi-dimensional EEG feature fusion and optimization," *Biomed Signal Process Control*, vol. 83, p. 104657, 2023, doi: https://doi.org/10.1016/j.bspc.2023.104657.

[17] Y. Li, A. Liu, J. Yin, C. Li, and X. Chen, "A Segmentation-Denoising Network for Artifact Removal From Single-Channel EEG," *IEEE Sens J*, vol. 23, no. 13, pp. 15115–15127, 2023, doi: 10.1109/JSEN.2023.3276481.

[18] J. A. Urigüen and B. Garcia-Zapirain, "EEG artifact removal—state-of-the-art and guidelines," *J Neural Eng*, vol. 12, no. 3, p. 031001, 2015, doi: 10.1088/1741-2560/12/3/031001.

[19] K. T. Sweeney, T. E. Ward, and S. F. McLoone, "Artifact removal in physiological signals-practices and possibilities," *IEEE Transactions on Information Technology in Biomedicine*, vol. 16, no. 3, pp. 488–500, 2012, doi: 10.1109/TITB.2012.2188536.

[20] L. Vigon, M. Saatchi, J. E. W. Mayhew, and R. Fernandes, "Quantitative evaluation of techniques for ocular artefact filtering of EEG waveforms," 2000. [Online]. Available: https://api.semanticscholar.org/CorpusID:61818742

[21] S. Makeig, A. Bell, T.-P. Jung, and T. J. Sejnowski, "Independent Component Analysis of Electroencephalographic Data," in *Advances in Neural Information Processing Systems*, D. Touretzky, M. C. Mozer, and M. Hasselmo, Eds., MIT Press, 1995. [Online]. Available: https://proceedings.neurips.cc/paper_files/paper/1995/file/754dda4b1ba34c6fa89716b85d68532b-Paper.pdf

[22] P. Yuan, L. Jiang, J. Liu, D. Zhou, P. Li, and Y. Gao, "Dual-Level Attention Based on Heterogeneous Graph Convolution Network for Aspect-Based Sentiment Classification," in *2020 IEEE International Conference on Smart Cloud (SmartCloud)*, 2020, pp. 74–77. doi: 10.1109/SmartCloud49737.2020.00022.

[23] L. Jiang, J. Liu, D. Zhou, Q. Zhou, X. Yang, and G. Yu, "Predicting the Evolution of Hot Topics: A Solution Based on the Online Opinion Dynamics Model in Social Network," *IEEE Trans Syst Man Cybern Syst*, vol. 50, no. 10, pp. 3828–3840, 2020, doi: 10.1109/TSMC.2018.2876235.

[24] P. Senthil Kumar, R. Arumuganathan, K. Sivakumar, and C. Vimal, "Removal of Ocular Artifacts in the EEG through Wavelet Transform without using an EOG Reference Channel," 2008.

[25] N. Mammone, F. La Foresta, and F. C. Morabito, "Automatic Artifact Rejection From Multichannel Scalp EEG by Wavelet ICA," *IEEE Sens J*, vol. 12, no. 3, pp. 533–542, 2012, doi: 10.1109/JSEN.2011.2115236.

[26] N. E. Huang *et al.*, "The empirical mode decomposition and the Hilbert spectrum for nonlinear and non-stationary time series analysis," *Proceedings of the Royal Society of London. Series A: Mathematical, Physical and Engineering Sciences*, vol. 454, no. 1971, pp. 903–995, Mar. 1998, doi: 10.1098/rspa.1998.0193.

[27] Z. Wu and N. E. Huang, "Ensemble Empirical Mode Decomposition: a Noise-Assisted Data Analysis Method," *Adv Adapt Data Anal*, vol. 01, no. 01, pp. 1–41, 2009.

[28] M. E. Torres, M. A. Colominas, G. Schlotthauer, and P. Flandrin, "A complete ensemble empirical mode decomposition with adaptive noise," in *2011 IEEE International Conference on Acoustics, Speech and Signal Processing (ICASSP)*, 2011, pp. 4144–4147. doi: 10.1109/ICASSP.2011.5947265.

[29] M. A. Colominas, G. Schlotthauer, and M. E. Torres, "Improved complete ensemble EMD: A suitable tool for biomedical signal processing," *Biomed Signal Process Control*, vol. 14, no. 1, pp. 19–29, 2014, doi: 10.1016/j.bspc.2014.06.009.

[30] A. Mayeli, V. Zotev, H. Refai, and J. Bodurka, "Real-time EEG artifact correction during fMRI using ICA," *J Neurosci Methods*, vol. 274, pp. 27–37, 2016, doi: https://doi.org/10.1016/j.jneumeth.2016.09.012.

[31] F. Esposito *et al.*, "Real-time independent component analysis of fMRI time-series," *Neuroimage*, vol. 20, no. 4, pp. 2209–2224, 2003, doi: https://doi.org/10.1016/j.neuroimage.2003.08.012.

[32] J. Onton, M. Westerfield, J. Townsend, and S. Makeig, "Imaging human EEG dynamics using independent component analysis," *Neurosci Biobehav Rev*, vol. 30, no. 6, pp. 808–822, 2006, doi: https://doi.org/10.1016/j.neubiorev.2006.06.007.

[33] C. Liu and C. Zhang, "Remove Artifacts from a Single-Channel EEG Based on VMD and SOBI," *Sensors*, vol. 22, no. 17, Sep. 2022, doi: 10.3390/s22176698.

[34] P. Flandrin, G. Rilling, and P. Gonçalvés, "Empirical mode decomposition as a filter bank," *IEEE Signal Process Lett*, vol. 11, no. 2 PART I, pp. 112–114, 2004, doi: 10.1109/LSP.2003.821662.

[35] N. E. Huang *et al.*, "The empirical mode decomposition and the Hilbert spectrum for nonlinear and non-stationary time series analysis," *Proceedings of The Royal Society A: Mathematical, Physical and Engineering Sciences*, vol. 454, no. 1971, pp. 903–995, 1998.

[36] R. Deering and J. F. Kaiser, "The use of a masking signal to improve empirical mode decomposition," in *Proceedings. (ICASSP '05). IEEE International Conference on Acoustics, Speech, and Signal Processing, 2005.*, 2005, p. iv/485-iv/488 Vol. 4. doi: 10.1109/ICASSP.2005.1416051.

[37] F. F. Tsai, S. Z. Fan, Y. S. Lin, N. E. Huang, and J. R. Yeh, "Investigating power density and the degree of nonlinearity in intrinsic components of anesthesia EEG by the hilbert-huang transform: An example using ketamine and alfentanil," *PLoS One*, vol. 11, no. 12, pp. 1–17, 2016, doi: 10.1371/journal.pone.0168108.

[38] K. T. Nguyen *et al.*, "Unraveling nonlinear electrophysiologic processes in the human visual system with full dimension spectral analysis," *Sci Rep*, vol. 9, no. 1, p. 16919, 2019, doi: 10.1038/s41598-019-53286-z.

[39] C.-H. Juan *et al.*, "Revealing the Dynamic Nature of Amplitude Modulated Neural Entrainment With Holo-Hilbert Spectral Analysis," *Front Neurosci*, vol. 15, p. 977, 2021, doi: 10.3389/fnins.2021.673369.

[40] M. A. Klados and P. D. Bamidis, "A semi-simulated EEG/EOG dataset for the comparison of EOG artifact rejection techniques," 2016, doi: 10.1109/JSEN.

[41] M. Dora and D. Holcman, “Adaptive Single-Channel EEG Artifact Removal with Applications to Clinical Monitoring,” *IEEE Transactions on Neural Systems and Rehabilitation Engineering*, vol. 30, pp. 286–295, 2022, doi: 10.1109/TNSRE.2022.3147072.